Title

Genetic deletion or pharmacological inhibition of soluble epoxide hydrolase attenuated particulate matter 2.5 exposure mediated lung injury

Authors

Zhang, Juan

Zhang, Wen-Hao

Morisseau, Christophe

et al.

Publication Date

2023-09-01

DOI

10.1016/j.jhazmat.2023.131890

Peer reviewed

HHS Public Access

Author manuscript

J Hazard Mater. Author manuscript; available in PMC 2024 September 15.

Published in final edited form as:

J Hazard Mater. 2023 September 15; 458: 131890. doi:10.1016/j.jhazmat.2023.131890.

Genetic deletion or pharmacological inhibition of soluble epoxide hydrolase attenuated particulate matter 2.5 exposure mediated lung injury

Juan Zhang[a,c,+], **Wen-Hao Zhang**[a,b,+], **Christophe Morisseau**[d,+], **Min Zhang**[a,b], **Hong-Jun Dong**[a], **Qi-Meng Zhu**[a,b], **Xiao-Kui Huo**[a], **Cheng-Peng Sun**[a,b,e,*], **Bruce D. Hammock**[d,*], **Xiao-Chi Ma**[a,*]

[a]Second Affiliated Hospital, Dalian Medical University, Dalian 116044, People's Republic of China.

[b]College of Pharmacy, Dalian Medical University, Dalian 116044, People's Republic of China.

[c]School of Pharmaceutical Sciences, Medical School, Shenzhen University, Shenzhen 518061, People's Republic of China.

[d]Department of Entomology and Nematology, UC Davis Comprehensive Cancer Center, University of California, Davis, CA 95616, United States.

[e]School of Chinese Materia Medica, State Key Laboratory of Component-Based Chinese Medicine, Tianjin State Key Laboratory of Modern Chinese Medicine, Tianjin University of Traditional Chinese Medicine, Tianjin 301617, People's Republic of China

Abstract

Air pollution represented by particulate matter 2.5 (PM2.5) is closely related to diseases of the respiratory system. Although the understanding of its mechanism is limited, pulmonary inflammation is closely correlated with PM2.5-mediated lung injury. Soluble epoxide hydrolase (sEH) and epoxy fatty acids play a vital role in the inflammation. Herein, we attempted to use the metabolomics of oxidized lipids for analyzing the relationship of oxylipins with lung injury in a PM2.5-mediated mouse model, and found that the cytochrome P450 oxidases/sEH mediated metabolic pathway was involved in lung injury. Furthermore, the sEH overexpression was revealed in lung injury mice. Interestingly, sEH genetic deletion or the selective sEH inhibitor TPPU increased levels of epoxyeicosatrienoic acids (EETs) in lung injury mice, and inactivated pulmonary macrophages based on the MAPK/NF-κB pathway, resulting in protection against PM2.5-mediated lung injury. Additionally, a natural sEH inhibitor luteolin from *Inula japonica* displayed a pulmonary protective effect towards lung injury mediated by PM2.5 as well. Our results are consistent with the sEH message and protein being both a marker and mechanism for PM2.5-induced inflammation, which suggest its potential as a pharmaceutical target for treating diseases of the respiratory system.

[*]Cheng-Peng Sun, Bruce D. Hammock, and Xiao-Chi Ma, suncp146@163.com (C.P. Sun); bdhammock@ucdavis.edu (B.D. Hammock); maxc1978@163.com (X.C. Ma).

[+]These authors contributed equally to this work.

Declaration of Competing Interest

The authors declare no competing financial interest.

Keywords

PM2.5; polyunsaturated fatty acids; soluble epoxide hydrolase; lung injury

1. Introduction

Recently, air pollution has become an increasingly serious problem due to the rapid industrialization and urbanization (Liu et al., 2022; Yao et al., 2020). Exposure to air pollution is associated with various diseases, particularly respiratory infections and cardiopulmonary diseases. These are, at least in part, attributed to particulate matter (PM) (Bowe et al., 2019; Cui et al., 2020). PM2.5 is characterized by the combustion of organic matter, fuels, and wastes with a diameter less than 2.5 μm, and its main sources are from vehicle exhaust, industry, power plants, and fireplaces (Aryal et al., 2021). Emerging evidence demonstrates that PM2.5 exposure not only reduces life expectancy, but also increases the incidence of diseases, including respiratory diseases, diabetes mellitus, and even neurologic diseases (Leclercq et al., 2017). For example, PM2.5 penetrates into the respiratory airway and deposits in the respiratory bronchiole and alveoli. These areas of the lung are difficult to clear effectively, contributing to respiratory system diseases, such as asthma, lung injury, and chronic obstructive pulmonary disease (COPD) (Valavanidis et al., 2013). In the respiratory system, the activation of alveolar macrophages stimulated by PM2.5, loaded with a variety of metal particle, organic pollutants, bacteria, fungi, and viruses, leads to the production of abundant inflammatory mediators (e.g. IL-1β, IL-6, and TNF-α), followed by the recruitment of neutrophiles, allowing the unbalance of the pro-inflammatory and anti-inflammatory factors to damage the respiratory tract, especially lung (Jia et al., 2021; Zhou et al., 2020). Therefore, modulating and resolving the inflammation functions as a vital tactics for treating PM2.5-mediated lung injury.

Polyunsaturated fatty acids (PUFAs) belong to a family of straight-chain fatty acids with 18 or more carbon atoms and 2–6 double bonds, and are classified into two types, based on the position of the omega terminal olefin including ω−3 (e.g. α-linolenic acid (ALA), docosahexaenoic acid (DHA), and eicosapentaenoic acid (EPA)) and ω−6 (e.g. dihomo-gamma-linolenic acid (DGLA), and arachidonic acid (AA)) (Lee et al., 2016). PUFAs are essential for eukaryotic cell membranes where they maintain the relative fluidity of cell membrane, thereby impart desirable physiological properties of cells (Qiu et al., 2020). PUFAs as the important precursors to signal molecules modulate various physiological processes in humans and animals, including neural development, immunity, and brain maturation (de Urquiza et al., 2000; Gabbs et al., 2015; Janssen and Kiliaan, 2014). PUFAs are released from the phospholipids of cells mainly hydrolyzed by phospholipase A2 (PLA2) when the cell membrane is stimulated or an inflammatory response occurs (Wang et al., 2019). As a twenty-carbon PUFA, AA is the precursor of pro-inflammatory eicosanoids produced by cyclooxygenase (COX) and lipoxygenase (LOX), such as prostaglandins, prostacyclins, and leukotrienes. Nevertheless, epoxyeicosatrienoic acids (EETs), produced from AA under the action of cytochrome P450 oxidases, play a series of beneficial effects, especially their anti-inflammatory, antihypertensive, and analgic effects (An et al., 2021; Sun et al., 2021a; Wang et al., 2021c). EETs exert a suppression on the enzymatic activity of IκB

kinases to block the IκB degradation, resulting in the inactivation of nuclear transcription factors responsible for cytokine-mediated inflammation, and thus exert an anti-inflammatory effect (Node et al., 1999; Wang et al., 2021a). However, EETs can be readily hydrolyzed by soluble epoxide hydrolase enzyme (sEH) to dihydroxycosacictrienoic acids (DHETs) with decreased or no biological activities (Imig, 2019). sEH (genetic name, *Ephx2*), contains 555 amino acid residues with a C-terminal hydrolase function that is in charge of hydrolysis of epoxy fatty acids (EpFAs) (Garcia et al., 2019; Gomez et al., 2004; Sun et al., 2021a). A series of previous studies demonstrate the relationship of sEH and inflammation-related diseases, such as inflammatory pain, central nervous system (CNS) deterioration, and allergic airway disease (Dileepan et al., 2019; Fishbein et al., 2020; Harris and Hammock, 2013; Jones et al., 2019; Wu et al., 2019). *Ephx2* genetic knockout (KO) or pharmacological inhibition of sEH by kurarinone, TPPU, or PTUPB led to a decreased of symptom in the inflammation in acute lung injury (ALI) and CNS diseases (Ren et al., 2018; Sun et al., 2021b; Sun et al., 2022b; Yang et al., 2020). Therefore, sEH serves as a potential target of treating inflammation-related diseases.

In the current study, we attempted to assess the potential mechanism of PM2.5-mediated lung injury and the sEH enzyme as a potential target for pharmacological intervention. To understand how PM2.5 mediates inflammation in mice with lung injury, we evaluated the metabolomic profile of oxidized lipids (oxylipins), such as EETs, DHETs, epoxyeicosatetraenoic acids (EpETEs), and dihydroxyeicosatetraenoic acids (DHETEs), indicating the role of sEH in combination with other biochemical pathways. Using sEH KO mice and a classic sEH inhibitor TPPU, we examined the role of sEH in the activation of macrophages, and inflammatory response in the lung of PM2.5-exposed mice. In addition, we found a natural sEH inhibitor luteolin from *Inula japonica* Thunb. and applied it to attenuate the pathogenesis of lung injury in PM2.5-exposed mice.

2. Materials and Methods

2.1 Materials

The primary antibodies COX-2, p65, p-p38, p38, JNK, p-ERK, sEH, p-JNK, p-p65, GAPDH, MCP-1, and ERK were purchased from Affinity (Cincinnati, USA), Abcam (Massachusetts, USA), Abclonal (Wuhan, China), Proteintech (Wuhan, China) and Cell Signaling Technology (CST, Danvers, MA, USA), respectively. PM2.5 (SRM2786) was purchased from National Institute of Standards and Technology (Gaithersburg, MD, United States) and its detailed information was showed at https://tsapps.nist.gov/srmext/certificates/2786.pdf.

2.2 Plant material and extract preparation

Based on the result of bioactive-guided separation, the 80% ethanol extraction of *I. japonica* was isolated by preparative HPLC (40%−70% MeOH) to afford luteolin, and its structure was determined by NMR and HRMS spectra (Figures S9–11). The biotin-coupled luteolin (Bio-luteolin) was synthesized as the previous method (Liao et al., 2017), and determined by 1D and 2D NMR and HRMS spectra (Figures S12–16).

2.3 Animals

C57BL/6 wild-type (WT) and sEH KO mice (21–24 g, 8 weeks, male) were purchased from the Experimental Animal Center of Dalian Medical University (Dalian, China) and Cyagen Biosciences Inc. (Guangzhou, China), respectively. All animal experiments were performed based on the requirement of the Institutional Animal Care and Use Committee of Dalian Medical University.

2.4 Experimental procedure

First, C57BL/6 mice were divided into the control and PM2.5 groups (8 mice/group). Mice were administrated with the vehicle or PM2.5 (2.5 mg/kg, dissolved in saline) for 2 weeks (three times each week) by the intratracheal infusion (i.i.).

Second, C57BL/6 mice were randomly divided into the control group, TPPU (3 mg/kg, dissolved in 10% hydroxypropyl-β-cyclodextrin) group, PM2.5 group, and PM2.5 + TPPU (3 mg/kg) group (10 mice/group). Mice in the TPPU and PM2.5 + TPPU groups were administrated intragastrically with TPPU for three weeks, and treated with PM2.5 or the corresponding vehicle for 2 weeks (three times each week, from 1^{th} week to 2^{th} week) by the intratracheal infusion (i.i.). Mice in the control and PM2.5 groups were administrated with the vehicle or PM2.5.

Third, WT and sEH KO mice were randomly divided into the control WT group, the PM2.5-treated WT group, the control KO group, and the PM2.5-treated KO group (10 mice/group). Mice were administrated with the vehicle or PM2.5 for 2 weeks (three times each week).

Forth, C57BL/6 mice were divided into the control group, luteolin (20 mg/kg, dissolved in 10% hydroxypropyl-β-cyclodextrin) group, PM2.5 group, and PM2.5 + luteolin (20 mg/kg) group (10 mice/group). Mice in the luteolin and PM2.5 + luteolin groups were administrated intragastrically with luteolin for three weeks, and were treated with PM2.5 or the corresponding vehicle for 2 weeks (three times each week, from 1^{th} week to 2^{th} week) by the intratracheal infusion (i.i.). Mice in the control and PM2.5 groups were treated with the vehicle or PM2.5. Levels of TNF-α, IL-6, MPO, and LDH in lung samples were determined by their corresponding kit.

2.5 Cell culture and treatment

RAW264.7 cells were cultured in DMEM containing 10% FBS in a humidified incubator (37 °C, 5% CO_2). Cells were plated in the 96-well or 6-well plate overnight, treated with PM2.5 (0, 25, 50, and 100 μg/mL) as previously described (Li et al., 2020; Xia et al., 2017). After 24 h, the supernatants and cells were collected and used for determination levels of TNF-α, IL-6, and NO, and Western blot. All the experiments were conducted for three times.

2.6 LC-MS/MS analysis

Levels of EETs and DHETs in lung samples were determined by LC-MS/MS based on the previous methods (Liu et al., 2019a; Sun et al., 2022b; Zhao et al., 2020).

2.7 Oxylipin metabolomics

The lungs in the control and PM2.5 groups were homogenized with MeOH and extracted with EtOAc (3 times). Levels of oxylipin in suspension were analyzed by LC-MS/MS as previously described (Ren et al., 2018; Zhang et al., 2022a).

2.8 Western blot analysis

RAW264.7 cells and lung tissues were washed by cold PBS for 3 times and added to the lysis buffer containing 1% cocktail and 1% PMSF on ice for 30 min. Samples containing 30–40 μg of proteins were separated by SDS-PAGE on 10% gel electrophoresis and transferred onto PVDF membranes. The blocked membranes were incubated with mentioned primary antibodies at 4 °C overnight. The membranes were washed with TBST, incubated by secondary antibody, and then analyzed by the Tanon 5200-ECL detection system.

2.9 Immunohistochemistry staining

The fixed lungs of mice by 4% paraformaldehyde (Solarbio, Beijing, China) were embedded with paraffin, cut into 4 μm of sections, stained with an H&E kit and CD68 and sEH antibodies (Zhang et al., 2022a; Zhang et al., 2022b), and then analyzed by a Leica DM4B microscope (Leica, Germany).

2.10 sEH activity assessment

The inhibitory effect of luteolin was determined as described using substrate PHOME (Liu et al., 2019b; Morisseau and Hammock, 2007; Sun et al., 2020; Sun et al., 2022a; Sun et al., 2022b; Zhang et al., 2022a).

2.11 Fluorescence-based binding assay

Human recombinant sEH were pre-incubated with luteolin (0.1 μM) for 2 min, and the fluorescence signal was measured by a microplate reader. The dissociation constant (K_d) of luteolin with sEH was fitted as the previous method (Wang et al., 2021b).

2.12 Statistical analysis

All data were analyzed using GraphPad Prism 8 (GraphPad Software Inc., San Diego, CA, USA) with the method of t-test, one-way, or two-way ANOVA, and difference was considered significant if p-value was less than 0.05. Results were presented as means ± SEM.

3. Results

3.1 PM2.5 exposure induces the inflammation through the MAPK/NF-κB signaling pathway in vivo and in vitro

We detected the size and constituents of PM2.5 (SRM2786, purchased from National Institute of Standards and Technology, Gaithersburg, MD, United States), and found that its mean size was 2.8 μm, and it mainly consisted of fluorene (0.20 mg/kg), fluoranthene (10.28 mg/kg), pyrene (8.01 mg/kg), chrysene (6.82 mg/kg), benzo[*b*]fluoranthene (7.51 mg/kg), aluminum (33480 mg/kg), chromium (462.3 mg/kg), copper (847 mg/kg), manganese (780

mg/kg), etc., without endotoxins based on its certificate of analysis (https://tsapps.nist.gov/srmext/certificates/2786.pdf). Firstly, we investigated whether PM2.5 exposure could affect the pulmonary function through the experiment that mice were administrated with intratracheal instillation of PM2.5 (2.5 mg/kg, Figure 1A). Compared with the control group, PM2.5 exposure resulted in hyperemia and edema of the lung (Figure 1B). Furthermore, the alveolar wall thickness was increased, the alveoli collapsed and the activation of macrophages were observed through CD68 staining in PM2.5-exposed lung (Figures 1C and D). Levels of TNF-α and IL-6 in the lung were significantly enhanced after PM2.5 exposure as well as the increase of MPO and LDH activities (Figure 1E). MAPK and NF-κB serve as important transcription factors involved in regulating cellular responses to inflammation. By Western blot analysis, we further found their activation due to increasing of phosphorylated levels of p65, JNK, ERK, and p38 in the lung of mice treated with PM2.5, driving the increase of their downstream target proteins, such as COX-2 and MCP-1 (Figures 1F and G). Similarly, PM2.5 challenge promoted the release of inflammatory biomarkers TNF-α, IL-6, and nitric oxide (NO), and activated the MAPK/NF-κB signaling pathway in RAW264.7 cells in a dose-dependent manner (Figure 2). These results demonstrated that PM2.5 stimulated the inflammation via activating the MAPK/NF-κB signaling pathway, finally resulting in the lung injury.

3.2 Oxylipin metabolomic analysis demonstrated the role of sEH in PM2.5 exposure-mediated lung injury

Recently, metabolomics has rapidly evolved into a key technique in many research fields and is beneficial to early diagnose and treat diseases, and discover potentially metabolic pathways (Kalim and Rhee, 2017; Weiss and Kim, 2011). Therefore, we used metabolomics to analyze effects of PM2.5 towards oxylipins in the lung of mice (Tables S1 and S2). The orthogonal partial least squares-discriminant analysis (OPLS-DA) showed remarkable clustering and a large difference between the control and PM2.5 groups (Figure S1). We identified 16 differential metabolites between the control and PM2.5 groups as described in the volcano plot map (Figure 3A), including 6 upregulated and 10 downregulated metabolites in lung tissue. As shown in Figure 3B, the heatmap reflected differential metabolites more intuitively. The heat map demonstrated that three pairs of differential metabolites were observed, such as 11,12-EET, 14, 15-EET, and 17,18-EpETE and their corresponding diols 11,12-DHET, 14, 15-DHET, and 17,18-DHETE. Analysis of these differential metabolites revealed that PM2.5-mediated lung injury was associated with Cyp-sEH mediated AA and eicosapentaenoic acid (EPA) metabolism (Figure 3C), because PM2.5 challenge decreased levels of 11,12-EET, 14, 15-EET, and 17,18-EpETE, while increasing levels of their corresponding diols (Figure 3D). The ratio of epoxides and their diols (e.g. 11,12-EET/11,12-DHET, 14,15-EET/14,15-DHET, and 17,18-EpETE/17,18-DHETE) demonstrated the increase of the sEH activity in PM2.5-mediated lung injury (Figure 3D). Western blot result showed that PM2.5 exposure upregulated the sEH expression in the lung of mice (Figure 3E), which was further supported by the sEH staining (Figure 3F). Enhancement of sEH expression induced by PM2.5 exposure has also been demonstrated at the cellular level (Figures 3H and S2). Our experiments also proved that Cyp450 oxidases, such as Cyp2j5, Cyp2j8, Cyp2j9, and Cyp2c37–39, showed no significant change in their mRNA levels, while the *Ephx2* mRNA level was

significantly upregulated (Figure 3G). These correlations reveal an important role of sEH in the pulmonary inflammation resulting by PM2.5 exposure.

3.3 Inhibiting sEH by TPPU attenuated lung injure in vivo

To further test the relationship between PM2.5-exposed lung injury and sEH, we selected a sEH inhibitor TPPU for follow-up experiments. As depicted in Figure 4A, H&E staining analysis showed TPPU treatment reversed hyperemia, edema, the increasing of the alveolar wall thickness and the macrophage activation in PM2.5-mediated lung injury mice (Figure 4A). Similarly, TPPU administration reduced levels of TNF-α, IL-6, MPO, and LDH in the lung of mice treated with PM2.5 (Figures 4B and S3), and reversed the PM2.5-induced decrease of the substrates of sEH 8,9-EET, 11,12-EET, and 14,15-EET, while decreasing levels of their corresponding diols (Figures 4C and D). Notably, the ratio of EETs and DHETs was significantly increased in PM2.5-mediated lung injury mice after administration of TPPU (Figure 4E), demonstrating the inhibition of sEH. Moreover, Western blot data revealed that multiple inflammation-related pathways were markedly suppressed in PM2.5-mediated mice after TPPU treatment, including COX-2, MCP-1, p-p65, p-JNK, p-ERK, and p-p38 (Figures 4E and S4). These findings suggested that chemical inhibition of sEH could attenuate the inflammation in PM2.5-mediated lung injury.

3.4 sEH knockout attenuated PM2.5-induced lung injury

To further explain the effect of sEH in PM2.5-induced lung injury, sEH genetic KO mouse was constructed by removing four exons (from exon 2 to exon 5, Figure 5A). As shown in Figure 5B, *Ephx2* genetic deletion attenuated PM2.5-mediated pulmonary hyperaemia and edema. Furthermore, sEH genetic KO reduced the increasing of the alveolar wall thickness and the macrophage activation (Figures 5C and D) This effect was further supported by levels of biomarkers MPO, LDH, IL-6, and TNF-α (Figure 5E). Similarly, we observed downregulation of proteins involved in MAPKs and NF-κB pathway, which revealed the inhibition of the MAPK/NF-κB in PM2.5-induced *Ephx2*$^{-/-}$ mice (Figures 5F and G). These results strongly supported the protective effect of sEH deletion towards PM2.5-mediated lung injury.

3.5 Discovery of a natural sEH inhibitor luteolin and its application in PM2.5-mediated lung injury

Traditional Chinese medicines, such as *I. japonica*, *Alisma orientale*, and *Sophora flavescens*, function as a vital role for treating diseases. Therefore, we sought to discover sEH inhibitors from these natural products. Because of a significant inhibitory effect of the extract of *I. japonica* towards sEH, we constructed pharmacodynamic plot for it in order to uncover potential sEH inhibitors (Figure 6A). Based on the bioactivity-guided fractionation, luteolin (Figure 6B) was isolated and identified through ^{1}H and ^{13}C NMR and HRMS spectra (Figures S9–11). Luteolin inhibited the sEH activity with an IC_{50} and K_d value of 5.20 and 3.81 μM, based on the experiments of sEH-mediated substrate PHOME hydrolysis and the fluorescence-based binding assay (Figures 6C and D), respectively. In order to co-localization analysis of the binding of luteolin and sEH, we synthesized biotinylated luteolin (Bio-luteolin, Figures 6E and S12–16), and the immunofluorescent co-localization analysis revealed their direct binding (Figure 6F). For *in vivo* study, inhibition of sEH

by luteolin reversed PM2.5-mediated lung injury through reducing hyperemia, edema, the increasing of the alveolar wall thickness, the macrophage activation, and levels of MPO, LDH, IL-6, and TNF-α (Figures 6G and S5) through regulating some proteins expression involved in the MAPK/NF-κB pathway (Figures 6J and S6). Meanwhile, luteolin displayed an inhibitory effect towards sEH in PM2.5-exposed lung injury mice (Figures 6H, 6I, S7, and S8). These results suggested that luteolin served as a sEH inhibitor and pharmacological inhibition of sEH was a strategy to attenuate PM2.5-mediated lung injury.

4. Discussion

Ambient air pollution can pose serious threats to humans. This threat is illustrated by PM2.5 closely associated with various diseases, including asthma, respiratory infections and cardiopulmonary disease (Liu et al., 2022; Yao et al., 2020). In this study, we analyzed the effect of PM2.5 towards oxylipins by metabolomic analysis. The levels of EpFAs, such as 11,12-EET, 14,15-EET, and 17,18-EpETE, showed a negative correlation with lung injury mediated by PM2.5, and that the Cyp450 oxidases/sEH mediated metabolic pathway was involved in lung injury of the animal model induced by PM2.5. Meanwhile, the sEH overexpression was observed in the lung of PM2.5-exposed mice, which was further supported by its mRNA expression and the sEH immunostaining. Interestingly, sEH genetic deletion or chemical inhibition of sEH by TPPU protected against pulmonary hyperaemia and edema caused by PM2.5, and reduced the increasing of the alveolar wall thickness and collapse in PM2.5-treated mice. Furthermore, sEH KO or its pharmacological inhibition inactivated the macrophages via suppressing the MAPK/NF-κB pathway, exerting the protective effect against lung injury. In addition, we found that a natural sEH inhibitor luteolin from traditional Chinese medicine *I. japonica* showed a protective effect in lung injury exposed by PM2.5. Collectively, these findings demonstrated the role of sEH in PM2.5-mediated lung injury.

The industrial revolution bought improved clothing, food, shelter, and transportation. However, these industrial advances also led to adverse effects to the environment, such as air, water, and soil pollution (Rychlik et al., 2019; Wang et al., 2022). There is no doubt that the global environmental pollution is regarded as an international public health problem with multiple aspects (Garcia et al., 2019). Air pollution is one of the biggest public health issues throughout the world, and and may lead to the deaths of approximately 9 million people each year (Liu et al., 2022; Manisalidis et al., 2020; Yao et al., 2020). Increasing evidence has revealed that air pollution is closely associated with asthma, cough, wheezing, pulmonary insufficiency, and other respiratory diseases (Eze et al., 2014; Manisalidis et al., 2020). PM2.5 often transports various substances, including bacteria, viruses, heavy metals, and minerals (Zhou et al., 2020), and its exposure results in various respiratory diseases (e.g. pulmonary fibrosis) (Leclercq et al., 2017). Although its precise mechanism is still under study, the inflammation serves as a critical role in PM2.5-exposed lung injury. Jia et al. reported that PM2.5 activated the NLRP3 pathway to release inflammatory factors in the mouse model, resulting in the pulmonary inflammation (Jia et al., 2021). This work was supported by investigations focused on PM2.5-human bronchial epithelial cells 16HBE and macrophages (Jia et al., 2021; Xiong et al., 2021). A similar result was observed in clinical investigations on PM2.5 air pollution (Bowe et al., 2019; Cui et al., 2020). In our

study, exposure to PM2.5 resulted in pulmonary lesions and the infiltration of inflammatory cells, to activate the macrophages, followed by the inflammatory cascade via activating MAPK/NF-κB pathway. These findings illustrated the role of the inflammation in PM2.5-mediated pulmonary injury.

AA, a twenty-carbon PUFA, locates in cell membranes as phospholipids, is released to the cytoplasm under the PLA2 action when the cell membrane is stimulated or the inflammatory response occurs (Sun et al., 2021a; Wang et al., 2019). In the inflammatory response, the overexpression of COX-2 and LOX-5 results in the conversion of AA into pro-inflammatory prostaglandins and leukotrienes (Sun et al., 2021a; Wang et al., 2019). Furthermore, AA is metabolized by oxidases Cyp2j and Cyp2c to produce EpFAs, such as 14,15-EET, which brings remarkable physiological effects, including antihypertensive, and antalgic activities (An et al., 2021; Sun et al., 2021a; Wang et al., 2021c). Similarly, EpETEs, produced from a PUFA with two carbon chain and five double bonds EPA largely through the action of Cyp2j and Cyp2c, display pharmacological effects (Hara et al., 2022; Pu et al., 2020). Recent evidence has illustrated the role of EpFAs, such as EETs and EpETEs, in inflammation-medicated diseases, including autism, acute kidney injury (AKI), and pulmonary fibrosis (Deng et al., 2017; Pu et al., 2020; Sun et al., 2021b; Sun et al., 2022b; Zhao et al., 2020). Previous studies indicated that levels of EETs and EpETEs, such as 8,9-EET, 14,15-EET, and 8,9-EpETE, were decreased, and levels of their corresponding diols were increased in MPTP-mediated PD and amyloid beta (Aβ)-mediated AD mouse models (Ren et al., 2018; Sun et al., 2021b; Sun et al., 2022b). A similar result was reported in the hypoxia/reoxygenation (H/R)-caused AKI, and bleomycin-caused pulmonary fibrosis (Deng et al., 2017; Zhao et al., 2020). Herein, we used the metabolomics technology to analyze the relationship of oxylipins with PM2.5-mediated lung injury, and found the decreasing of levels of 11,12-EET, 14,15-EET, and 17,18-EpETE and the increasing of levels of their corresponding diols in lung injury resulting from PM2.5 exposure. These findings suggested the role of EpFAs in the inflammation for PM2.5-caused lung injury.

In our study, the decrease of EpFAs and the increase of their diols revealed that sEH was closely associated with PM2.5-mediated pulmonary injury. The sEH belongs to the family of α/β hydrolase fold proteins, and possesses the hydrolysis function of epoxides, such as EETs and EpETEs (Gomez et al., 2004; Sun et al., 2021a). Accumulating evidence suggests that sEH is overexpressed in inflammation-related diseases (e.g. inflammatory pain, AKI, and allergic airway disease) (Dileepan et al., 2019; Harris and Hammock, 2013; Jones et al., 2019; Ma et al., 2019; Ren et al., 2018; Sun et al., 2022b; Wang et al., 2020; Wu et al., 2019). The expression level of sEH was remarkably increased in the pulmonary inflammation of LPS-induced ALI and bleomycin-caused pulmonary fibrosis mouse models (Chen et al., 2020; Li et al., 2021; Yang et al., 2020; Zhang et al., 2023b; Zhang et al., 2022a; Zhao et al., 2020; Zhong et al., 2023), and its overexpression was reported in neuroinflammation of PD and AD (Ren et al., 2018; Sun et al., 2021b; Sun et al., 2022b). Similarly, the expression of sEH and its mRNA were higher than that of the control group in PM2.5-mediated mouse and RAW264.7 cell models. Furthermore, a sEH genetic deletion or its pharmacological inhibition by TPPU, alisol B, and kurarinone could stabilize levels of EETs to inactivate the NF-κB pathway, allowing the remission of inflammation (Chen et al., 2020; Deng et al., 2017; Pu et al., 2020; Ren et al., 2018; Sun et al., 2021b; Sun

et al., 2022b; Zhang et al., 2023a; Zhang et al., 2023b). Recently, PTUPB, a COX-2/sEH dual inhibitor, alleviated the pathological course of lung tissues, reduced the infiltration of inflammatory cells in an ALI animal model (Yang et al., 2020), which suggesting the key role of sEH in PM2.5-mediated pulmonary inflammation. In this study, *Ephx2* genetic KO and TPPU protected against pulmonary hyperaemia and edema, and blocked the macrophage activation through the MAPK/NF-κB pathway to attenuate the pulmonary inflammation in PM2.5-mediated lung injury. Additionally, we found that a natural sEH inhibitor luteolin from traditional Chinese medicine *I. japonica* displayed the pulmonary protective effect in PM2.5-mediated animal model. These findings suggested that sEH could function as a therapeutic target of PM2.5-caused pulmonary injury.

5. Conclusion

In summary, we found that the levels of oxylipins were significantly different in the lung of PM2.5-mediated and control mice, including 11,12-EET, 14,15-EET, and 17,18-EpETE, which showed a negative correlation with PM2.5-caused lung injury. Furthermore, sEH overexpression was observed in PM2.5-mediated mouse and cell models. It was worth noting that sEH genetic deletion or pharmacological inhibition of sEH by TPPU attenuated pulmonary hyperaemia and edema, and inhibited the MAPK/NF-κB pathway for the macrophage inactivation, leading to the protective effect against PM2.5-mediated lung injury. Additionally, a natural sEH inhibitor luteolin from traditional Chinese medicine *I. japonica* displayed a similar protective effect in the PM2.5-mediated mouse model. Therefore, these findings revealed that sEH could function as a therapeutic target of PM2.5-caused pulmonary injury.

Supplementary Material

Refer to Web version on PubMed Central for supplementary material.

Funding

This work is supported by National Natural Science Foundation of China (No. 82274069 and 81930112), Revolutionizing Innovative, Visionary Environmental Health Research Program of the National Institute of Environmental Health Sciences (No. R35 ES030443), Superfund Basic Research Program of the National Institutes of Environmental Health Sciences (No. P42 ES04699), China Postdoctoral Science Foundation (No. 2022M720095), and Young Elite Scientists Sponsorship Program by China Association of Chinese Medicine (No. 2022-QNRC2-B09).

References

An G, Lee KSS, Yang J, Hammock BD, 2021. Target-mediated drug disposition-a class effect of soluble epoxide hydrolase inhibitors. J Clin Pharmacol 61, 531–537. [PubMed: 33078430]

Aryal A, Harmon AC, Dugas TR, 2021. Particulate matter air pollutants and cardiovascular disease: Strategies for intervention. Pharmacol Ther 223, 107890. [PubMed: 33992684]

Bowe B, Xie Y, Yan Y, Al-Aly Z, 2019. Burden of cause-specific mortality associated with PM2.5 air pollution in the United States. JAMA Netw Open 2, e1915834.

Chen Z, Tang Y, Yu J, Dong R, Yang Y, Fu M, Luo J, Hu S, Wang DW, Tu L, Xu X, 2020. sEH Inhibitor Tppu Ameliorates Cecal Ligation and Puncture-Induced Sepsis by Regulating Macrophage Functions. Shock 53, 761–771. [PubMed: 31318834]

Cui X, Li Z, Teng Y, Barkjohn KK, Norris CL, Fang L, Daniel GN, He L, Lin L, Wang Q, Day DB, Zhou X, Hong J, Gong J, Li F, Mo J, Zhang Y, Schauer JJ, Black MS, Bergin MH, Zhang J, 2020. Association between bedroom particulate matter filtration and changes in airway pathophysiology in children with asthma. JAMA Pediatr 174, 533–542. [PubMed: 32250418]

de Urquiza AM, Liu S, Sjoberg M, Zetterstrom RH, Griffiths W, Sjovall J, Perlmann T, 2000. Docosahexaenoic acid, a ligand for the retinoid X receptor in mouse brain. Science 290, 2140–2144. [PubMed: 11118147]

Deng BQ, Luo Y, Kang X, Li CB, Morisseau C, Yang J, Lee KSS, Huang J, Hu DY, Wu MY, Peng A, Hammock BD, Liu JY, 2017. Epoxide metabolites of arachidonate and docosahexaenoate function conversely in acute kidney injury involved in GSK3beta signaling. Proc Natl Acad Sci U S A 114, 12608–12613. [PubMed: 29109264]

Dileepan M, Rastle-Simpson S, Greenberg Y, Wijesinghe DS, Kumar NG, Yang J, Hwang SH, Hammock BD, Sriramarao P, Rao SP, 2019. Effect of dual sEH/COX-2 inhibition on allergen-induced airway inflammation. Front Pharmacol 10, 1118. [PubMed: 31611798]

Eze IC, Schaffner E, Fischer E, Schikowski T, Adam M, Imboden M, Tsai M, Carballo D, von Eckardstein A, Kunzli N, Schindler C, Probst-Hensch N, 2014. Long-term air pollution exposure and diabetes in a population-based Swiss cohort. Environ Int 70, 95–105. [PubMed: 24912113]

Fishbein A, Wang W, Yang H, Yang J, Hallisey VM, Deng J, Verheul SML, Hwang SH, Gartung A, Wang Y, Bielenberg DR, Huang S, Kieran MW, Hammock BD, Panigrahy D, 2020. Resolution of eicosanoid/cytokine storm prevents carcinogen and inflammation-initiated hepatocellular cancer progression. Proc Natl Acad Sci U S A 117, 21576–21587. [PubMed: 32801214]

Gabbs M, Leng S, Devassy JG, Monirujjaman M, Aukema HM, 2015. Advances in our understanding of oxylipins derived from dietary PUFAs. Adv Nutr 6, 513–540. [PubMed: 26374175]

Garcia E, Urman R, Berhane K, McConnell R, Gilliland F, 2019. Effects of policy-driven hypothetical air pollutant interventions on childhood asthma incidence in southern California. Proc Natl Acad Sci U S A 116, 15883–15888. [PubMed: 31332016]

Gomez GA, Morisseau C, Hammock BD, Christianson DW, 2004. Structure of human epoxide hydrolase reveals mechanistic inferences on bifunctional catalysis in epoxide and phosphate ester hydrolysis. Biochemistry 43, 4716–4723. [PubMed: 15096040]

Hara S, Tojima I, Shimizu S, Kouzaki H, Shimizu T, 2022. 17,18-epoxyeicosatetraenoic acid inhibits TNF-alpha-induced inflammation in cultured human airway epithelium and LPS-induced murine airway inflammation. Am J Rhinol Allergy 36, 106–114. [PubMed: 34236247]

Harris TR, Hammock BD, 2013. Soluble epoxide hydrolase: gene structure, expression and deletion. Gene 526, 61–74. [PubMed: 23701967]

Imig JD, 2019. Epoxyeicosanoids in hypertension. Physiol Res 68, 695–704. [PubMed: 31475560]

Janssen CI, Kiliaan AJ, 2014. Long-chain polyunsaturated fatty acids (LCPUFA) from genesis to senescence: the influence of LCPUFA on neural development, aging, and neurodegeneration. Prog Lipid Res 53, 1–17. [PubMed: 24334113]

Jia H, Liu Y, Guo D, He W, Zhao L, Xia S, 2021. PM2.5-induced pulmonary inflammation via activating of the NLRP3/caspase-1 signaling pathway. Environ Toxicol 36, 298–307. [PubMed: 32996690]

Jones RD, Liao J, Tong X, Xu D, Sun L, Li H, Yang GY, 2019. Epoxy-oxylipins and soluble epoxide hydrolase metabolic pathway as targets for NSAID-induced gastroenteropathy and inflammation-associated carcinogenesis. Front Pharmacol 10, 731. [PubMed: 31293429]

Kalim S, Rhee EP, 2017. An overview of renal metabolomics. Kidney Int 91, 61–69. [PubMed: 27692817]

Leclercq B, Platel A, Antherieu S, Alleman LY, Hardy EM, Perdrix E, Grova N, Riffault V, Appenzeller BM, Happillon M, Nesslany F, Coddeville P, Lo-Guidice JM, Garcon G, 2017. Genetic and epigenetic alterations in normal and sensitive COPD-diseased human bronchial epithelial cells repeatedly exposed to air pollution-derived PM2.5. Environ Pollut 230, 163–177. [PubMed: 28651088]

Lee JM, Lee H, Kang S, Park WJ, 2016. Fatty acid desaturases, polyunsaturated fatty acid regulation, and biotechnological advances. Nutrients 8.

Li H, Bradbury JA, Edin ML, Graves JP, Gruzdev A, Cheng J, Hoopes SL, DeGraff LM, Fessler MB, Garantziotis S, Schurman SH, Zeldin DC, 2021. sEH promotes macrophage phagocytosis and lung clearance of Streptococcus pneumoniae. J Clin Invest 131.

Li M, Hua Q, Shao Y, Zeng H, Liu Y, Diao Q, Zhang H, Qiu M, Zhu J, Li X, Ling Y, Zhang R, Jiang Y, 2020. Circular RNA circBbs9 promotes PM(2.5)-induced lung inflammation in mice via NLRP3 inflammasome activation. Environ Int 143, 105976. [PubMed: 32707273]

Liao LX, Song XM, Wang LC, Lv HN, Chen JF, Liu D, Fu G, Zhao MB, Jiang Y, Zeng KW, Tu PF, 2017. Highly selective inhibition of IMPDH2 provides the basis of antineuroinflammation therapy. Proc Natl Acad Sci U S A 114, E5986–E5994. [PubMed: 28674004]

Liu G, Li Y, Zhou J, Xu J, Yang B, 2022. PM2.5 deregulated microRNA and inflammatory microenvironment in lung injury. Environ Toxicol Pharmacol 91, 103832. [PubMed: 35189342]

Liu Y, Liu Z, Wei M, Hu M, Yue K, Bi R, Zhai S, Pi Z, Song F, Liu Z, 2019a. Pharmacodynamic and urinary metabolomics studies on the mechanism of Schisandra polysaccharide in the treatment of Alzheimer's disease. Food Funct 10, 432–447. [PubMed: 30623955]

Liu ZB, Sun CP, Xu JX, Morisseau C, Hammock BD, Qiu F, 2019b. Phytochemical constituents from Scutellaria baicalensis in soluble epoxide hydrolase inhibition: Kinetics and interaction mechanism merged with simulations. Int J Biol Macromol 133, 1187–1193. [PubMed: 30980876]

Ma M, Ren Q, Yang J, Zhang K, Xiong Z, Ishima T, Pu Y, Hwang SH, Toyoshima M, Iwayama Y, Hisano Y, Yoshikawa T, Hammock BD, Hashimoto K, 2019. Key role of soluble epoxide hydrolase in the neurodevelopmental disorders of offspring after maternal immune activation. Proc Natl Acad Sci U S A 116, 7083–7088. [PubMed: 30890645]

Manisalidis I, Stavropoulou E, Stavropoulos A, Bezirtzoglou E, 2020. Environmental and health impacts of air pollution: A review. Front Public Health 8, 14. [PubMed: 32154200]

Morisseau C, Hammock BD, 2007. Measurements of soluble epoxide hydrolase (sEH) activity. Curr. Protoc. Toxicol 33, 4.23.21–24.23.18.

Node K, Huo Y, Ruan X, Yang B, Spiecker M, Ley K, Zeldin DC, Liao JK, 1999. Anti-inflammatory properties of cytochrome P450 epoxygenase-derived eicosanoids. Science 285, 1276–1279. [PubMed: 10455056]

Pu Y, Yang J, Chang L, Qu Y, Wang S, Zhang K, Xiong Z, Zhang J, Tan Y, Wang X, Fujita Y, Ishima T, Wang D, Hwang SH, Hammock BD, Hashimoto K, 2020. Maternal glyphosate exposure causes autism-like behaviors in offspring through increased expression of soluble epoxide hydrolase. Proc Natl Acad Sci U S A 117, 11753–11759. [PubMed: 32398374]

Qiu X, Xie X, Meesapyodsuk D, 2020. Molecular mechanisms for biosynthesis and assembly of nutritionally important very long chain polyunsaturated fatty acids in microorganisms. Prog Lipid Res 79, 101047. [PubMed: 32540152]

Ren Q, Ma M, Yang J, Nonaka R, Yamaguchi A, Ishikawa KI, Kobayashi K, Murayama S, Hwang SH, Saiki S, Akamatsu W, Hattori N, Hammock BD, Hashimoto K, 2018. Soluble epoxide hydrolase plays a key role in the pathogenesis of Parkinson's disease. Proc Natl Acad Sci U S A 115, E5815–E5823. [PubMed: 29735655]

Rychlik KA, Secrest JR, Lau C, Pulczinski J, Zamora ML, Leal J, Langley R, Myatt LG, Raju M, Chang RC, Li Y, Golding MC, Rodrigues-Hoffmann A, Molina MJ, Zhang R, Johnson NM, 2019. In utero ultrafine particulate matter exposure causes offspring pulmonary immunosuppression. Proc Natl Acad Sci U S A 116, 3443–3448. [PubMed: 30808738]

Sun CP, Zhang J, Zhao WY, Yi J, Yan JK, Wang YL, Morisseau C, Liu ZB, Hammock BD, Ma XC, 2020. Protostane-type triterpenoids as natural soluble epoxide hydrolase inhibitors: Inhibition potentials and molecular dynamics. Bioorg Chem 96, 103637. [PubMed: 32032849]

Sun CP, Zhang XY, Morisseau C, Hwang SH, Zhang ZJ, Hammock BD, Ma XC, 2021a. Discovery of soluble epoxide hydrolase inhibitors from chemical synthesis and natural products. J Med Chem 64, 184–215. [PubMed: 33369424]

Sun CP, Zhang XY, Zhou JJ, Huo XK, Yu ZL, Morisseau C, Hammock BD, Ma XC, 2021b. Inhibition of sEH via stabilizing the level of EETs alleviated Alzheimer's disease through GSK3beta signaling pathway. Food Chem Toxicol 156, 112516. [PubMed: 34411643]

Sun CP, Zhou JJ, Yu ZL, Huo XK, Zhang J, Morisseau C, Hammock BD, Ma XC, 2022a. Kurarinone alleviated Parkinson's disease via stabilization of epoxyeicosatrienoic acids in animal model. Proc Natl Acad Sci U S A 119, e2118818119.

Valavanidis A, Vlachogianni T, Fiotakis K, Loridas S, 2013. Pulmonary oxidative stress, inflammation and cancer: Respirable particulate matter, fibrous dusts and ozone as major causes of lung carcinogenesis through reactive oxygen species mechanisms. Int J Environ Res Public Health 10, 3886–3907. [PubMed: 23985773]

Wang B, Wu L, Chen J, Dong L, Chen C, Wen Z, Hu J, Fleming I, Wang DW, 2021a. Metabolism pathways of arachidonic acids: mechanisms and potential therapeutic targets. Signal Transduct Target Ther 6, 94. [PubMed: 33637672]

Wang KB, Dickerhoff J, Yang D, 2021b. Solution structure of ternary complex of berberine bound to a dGMP-fill-in vacancy G-quadruplex formed in the PDGFR-beta promoter. J Am Chem Soc 143, 16549–16555. [PubMed: 34586799]

Wang T, Fu X, Chen Q, Patra JK, Wang D, Wang Z, Gai Z, 2019. Arachidonic acid metabolism and kidney inflammation. International journal of molecular sciences 20.

Wang Y, Apte JS, Hill JD, Ivey CE, Patterson RF, Robinson AL, Tessum CW, Marshall JD, 2022. Location-specific strategies for eliminating US national racial-ethnic exposure inequality. Proc Natl Acad Sci U S A 119, e2205548119.

Wang Y, Wagner KM, Morisseau C, Hammock BD, 2021c. Inhibition of the soluble epoxide hydrolase as an analgesic strategy: A review of preclinical evidence. J Pain Res 14, 61–72. [PubMed: 33488116]

Wang Y, Yang J, Wang W, Sanidad KZ, Cinelli MA, Wan D, Hwang SH, Kim D, Lee KSS, Xiao H, Hammock BD, Zhang G, 2020. Soluble epoxide hydrolase is an endogenous regulator of obesity-induced intestinal barrier dysfunction and bacterial translocation. Proc Natl Acad Sci U S A 117, 8431–8436. [PubMed: 32220957]

Weiss RH, Kim K, 2011. Metabolomics in the study of kidney diseases. Nat Rev Nephrol 8, 22–33. [PubMed: 22025087]

Wu Q, Song J, Meng D, Chang Q, 2019. TPPU, a sEH inhibitor, attenuates corticosterone-induced PC12 cell injury by modulation of BDNF-TrkB pathway. J Mol Neurosci 67, 364–372. [PubMed: 30644034]

Xia WR, Fu W, Wang Q, Zhu X, Xing WW, Wang M, Xu DQ, Xu DG, 2017. Autophagy induced FHL2 upregulation promotes IL-6 production by activating the NF-kappaB pathway in mouse aortic endothelial cells after exposure to PM2.5. Inter J Mol Sci 18, 1484.

Xiong R, Jiang W, Li N, Liu B, He R, Wang B, Geng Q, 2021. PM2.5-induced lung injury is attenuated in macrophage-specific NLRP3 deficient mice. Ecotoxicol Environ Saf 221, 112433. [PubMed: 34146983]

Yang HH, Duan JX, Liu SK, Xiong JB, Guan XX, Zhong WJ, Sun CC, Zhang CY, Luo XQ, Zhang YF, Chen P, Hammock BD, Hwang SH, Jiang JX, Zhou Y, Guan CX, 2020. A COX-2/sEH dual inhibitor PTUPB alleviates lipopolysaccharide-induced acute lung injury in mice by inhibiting NLRP3 inflammasome activation. Theranostics 10, 4749–4761. [PubMed: 32308747]

Yao M, Weschler CJ, Zhao B, Zhang L, Ma R, 2020. Breathing-rate adjusted population exposure to ozone and its oxidation products in 333 cities in China. Environ Int 138, 105617. [PubMed: 32155513]

Zhang J, Luan ZL, Huo XK, Zhang M, Morisseau C, Sun CP, Hammock BD, Ma XC, 2023a. Direct targeting of sEH with alisol B alleviated the apoptosis, inflammation, and oxidative stress in cisplatin-induced acute kidney injury. Inter J Biol Sci 19, 294–310.

Zhang J, Zhang M, Huo XK, Ning J, Yu ZL, Morisseau C, Sun CP, Hammock BD, Ma XC, 2023b. Macrophage inactivation by small molecule wedelolactone via targeting sEH for the treatment of LPS-induced acute lung injury. ACS Cent Sci 9, 440–456. [PubMed: 36968547]

Zhang J, Zhang M, Zhang WH, Zhu QM, Huo XK, Sun CP, Ma XC, Xiao HT, 2022a. Total flavonoids of Inula japonica alleviated the inflammatory response and oxidative stress in LPS-induced acute lung injury via inhibiting the sEH activity: Insights from lipid metabolomics. Phytomedicine 107, 154380. [PubMed: 36150346]

Zhang J, Zhang M, Zhang WH, Zhu QM, Ning J, Huo XK, Xiao HT, Sun CP, 2022b. Total terpenoids of Inula japonica activated the Nrf2 receptor to alleviate the inflammation and oxidative stress in LPS-induced acute lung injury. Phytomedicine 107, 154377. [PubMed: 36116200]

Zhao WY, Luan ZL, Liu TT, Ming WH, Huo XK, Huang HL, Sun CP, Zhang BJ, Ma XC, 2020. Inula japonica ameliorated bleomycin-induced pulmonary fibrosis via inhibiting soluble epoxide hydrolase. Bioorg Chem 102, 104065. [PubMed: 32663670]

Zhong WJ, Liu T, Yang HH, Duan JX, Yang JT, Guan XX, Xiong JB, Zhang YF, Zhang CY, Zhou Y, Guan CX, 2023. TREM-1 governs NLRP3 inflammasome activation of macrophages by firing up glycolysis in acute lung injury. Int J Biol Sci 19, 242–257. [PubMed: 36594089]

Zhou Y, Ma J, Wang B, Liu Y, Xiao L, Ye Z, Fan L, Wang D, Mu G, Chen W, 2020. Long-term effect of personal PM2.5 exposure on lung function: A panel study in China. J Hazard Mater 393, 122457. [PubMed: 32151939]

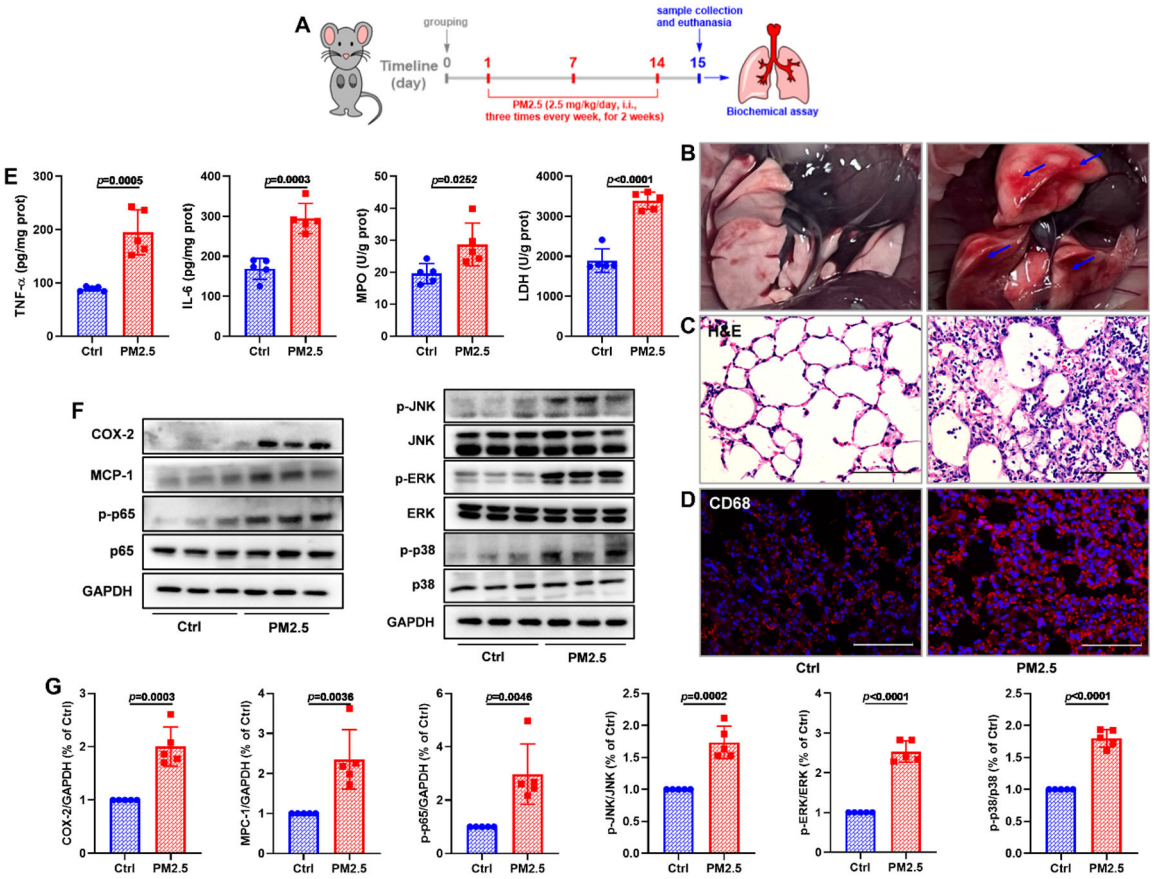

Figure 1. PM2.5 caused lung damage and inflammation in mice.

(A) The experimental procedure. (B) Representative lung plots. (C) Representative plots of H&E staining. (D) Representative plots of CD68 staining. (E) The content of TNF-α, IL-6, MPO, and LDH in mice treated with or without PM2.5 (2.5 mg/kg, mean ± SEM, n = 5, t-test). (F) Effects of PM2.5 to expressions of proteins related to NF-κB and MAPK signaling pathways. (G) Protein quantification of (F) (mean ± SEM, n = 5, t-test).

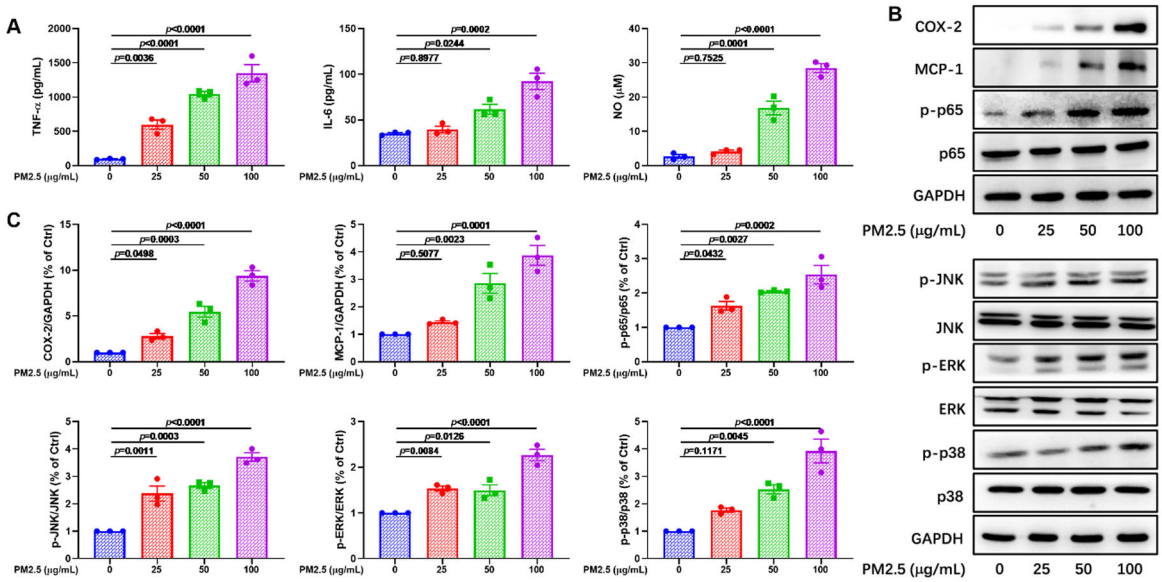

Figure 2. PM2.5 activated the MAPK/NF-κB signaling pathway to release inflammatory factors in RAW264.7 cells.

(A) TNF-a, IL-6, and NO were measured in conditioned medium in RAW264.7 cells treated with PM2.5 for 24 h (mean ± SEM, n = 3, one-way ANOVA). (B) Effects of PM2.5 to expressions of proteins related to MAPK/ NF-κB signaling pathways in RAW264.7 cells. (C) Quantification of (B) (mean ± SEM, n = 3, one-way ANOVA).

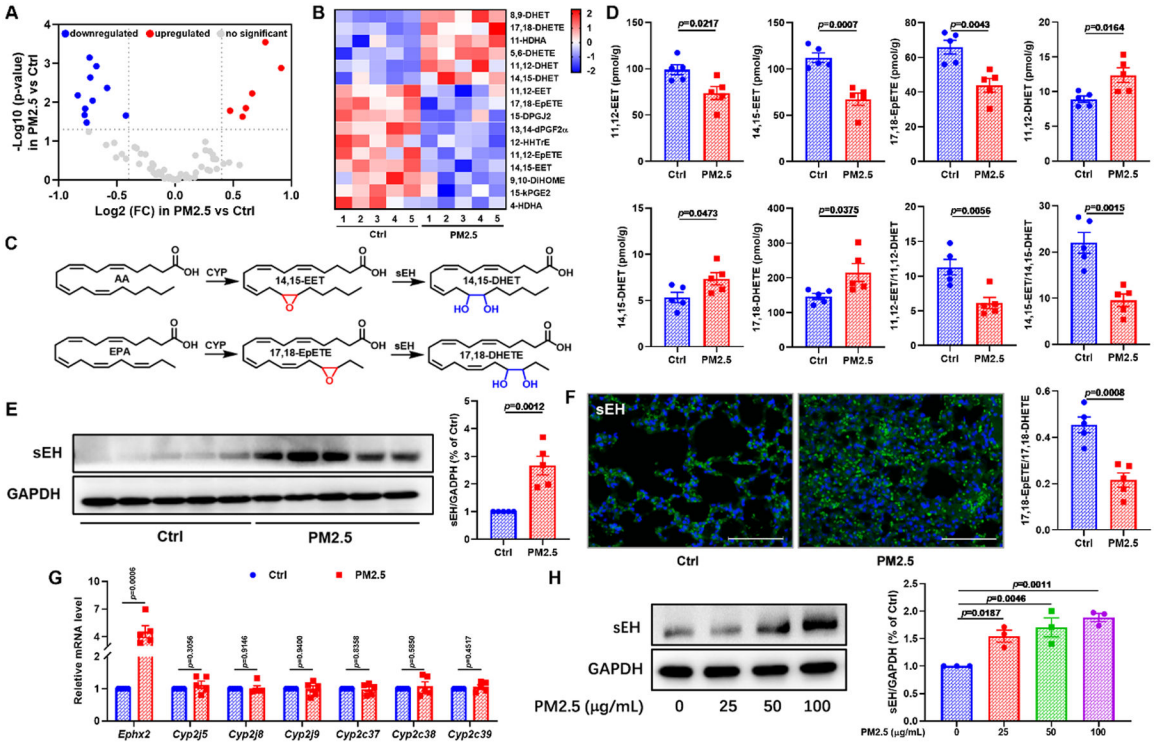

Figure 3. sEH served as a role in PM2.5-mediated lung injury.

(A) Volcano plot showing the differentially metabolites after PM2.5 exposure. (B) Heatmap plot. (C) The Cyp/sEH-medicated metabolism of AA. (D) Effects of PM2.5 on substrates and products of sEH. (E) Western blot analysis of sEH in the lung of mice after PM2.5 exposure (mean ± SEM, n = 5, t-test). (F) Representative plots of sEH staining. (G) PCR analysis of *Ephx2*, *Cyp2j5*, *Cyp2j8*, *Cyp2j9*, *Cyp2c37*, *Cyp2c38*, and *Cyp2c39* mRNA expressions in the lung of mice after PM2.5 exposure (mean ± SEM, n = 5, t-test). (H) Effects of PM2.5 to the sEH expression in RAW264.7 cells.

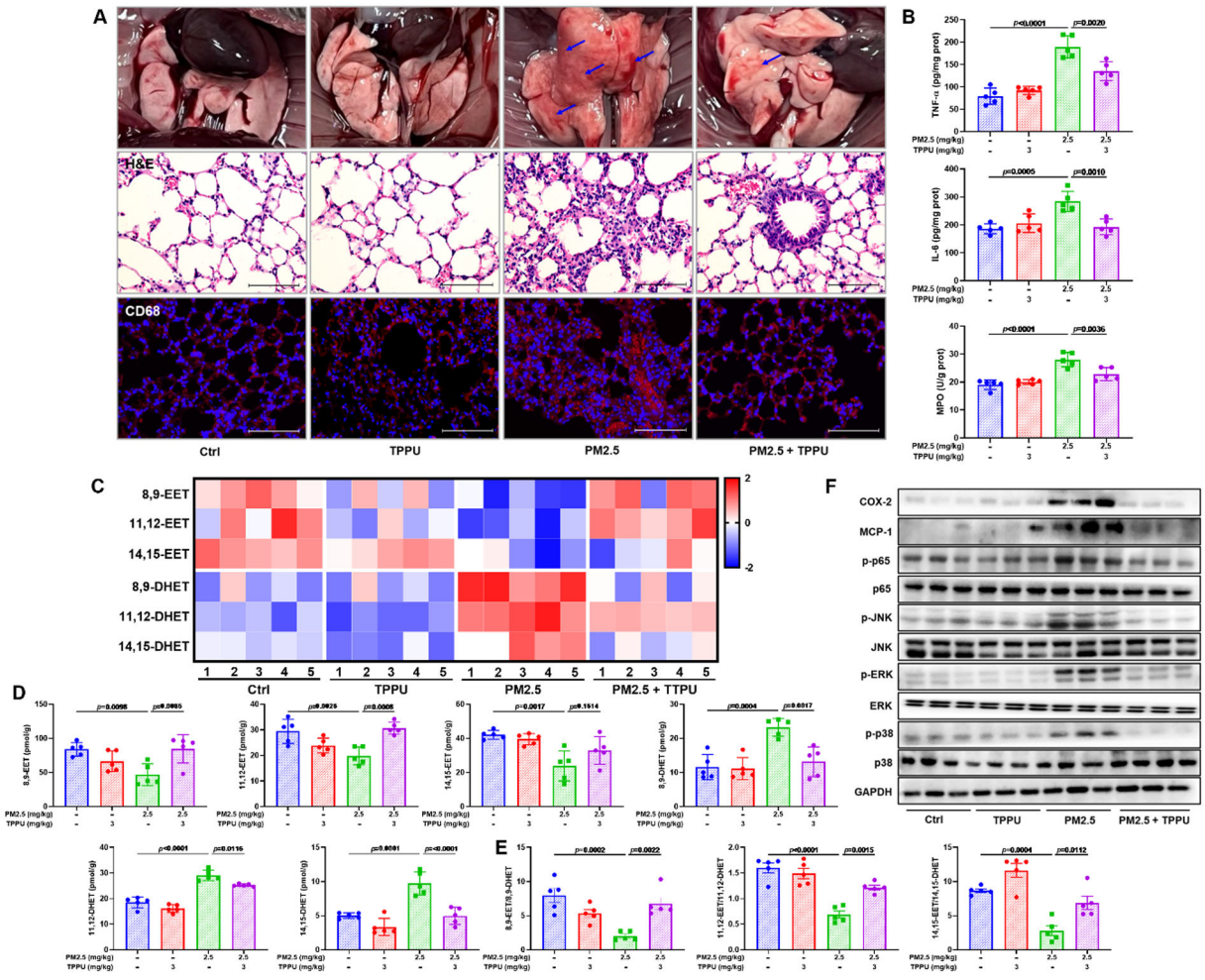

Figure 4. Inhibition of sEH by TPPU ameliorated PM2.5-mediated lung injury.

(A) Representative lung, H&E, and CD68 staining plots demonstrated that TPPU attenuated hyperemia and edema, and reduced the increasing of the alveolar collapse and the macrophage activation in PM2.5-mediated lung injury mice. (B) Effects of TPPU towards TNF-α, IL-6, and MPO in PM2.5 exposed mice (mean ± SEM, n = 5, one-way ANOVA). (C) Heatmap plot of substrates and products of sEH. (D) Effects of TPPU towards EETs and DHETs in PM2.5 exposed mice (mean ± SEM, n = 5, one-way ANOVA). (E) The ratio of EETs and DHETs (mean ± SEM, n = 5, one-way ANOVA). (F) Western blot analysis of proteins related to MAPK/ NF-κB signaling pathways in the PM2.5 induced mice after TPPU treatment.

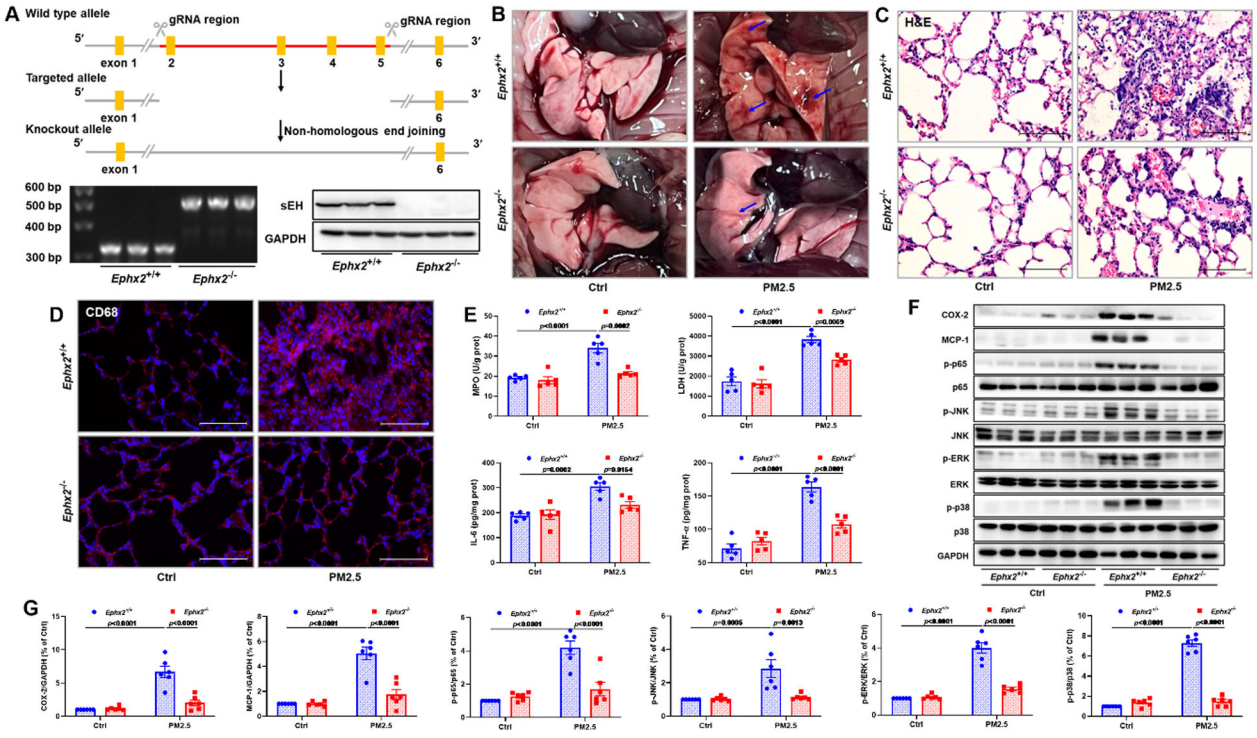

Figure 5. sEH KO attenuated of PM2.5 induced lung injury.

(A) The construction of sEH KO mice. (B-D) Representative lung, H&E, and CD68 staining plots. (E) Levels of MPO, LDH, IL-6, and TNF-α in PM2.5-mediated *Ephx2*$^{+/+}$ and *Ephx2*$^{-/-}$ mice (mean ± SEM, n = 5, two-way ANOVA). (F) Expression levels of proteins related to MAPK/ NF-κB signaling pathways in PM2.5-mediated *Ephx2*$^{+/+}$ and *Ephx2*$^{-/-}$ mice. (G) Quantitative data of expressions of (F) in PM2.5-mediated *Ephx2*$^{+/+}$ and *Ephx2*$^{-/-}$ mice (mean ± SEM, n = 6, two-way ANOVA).

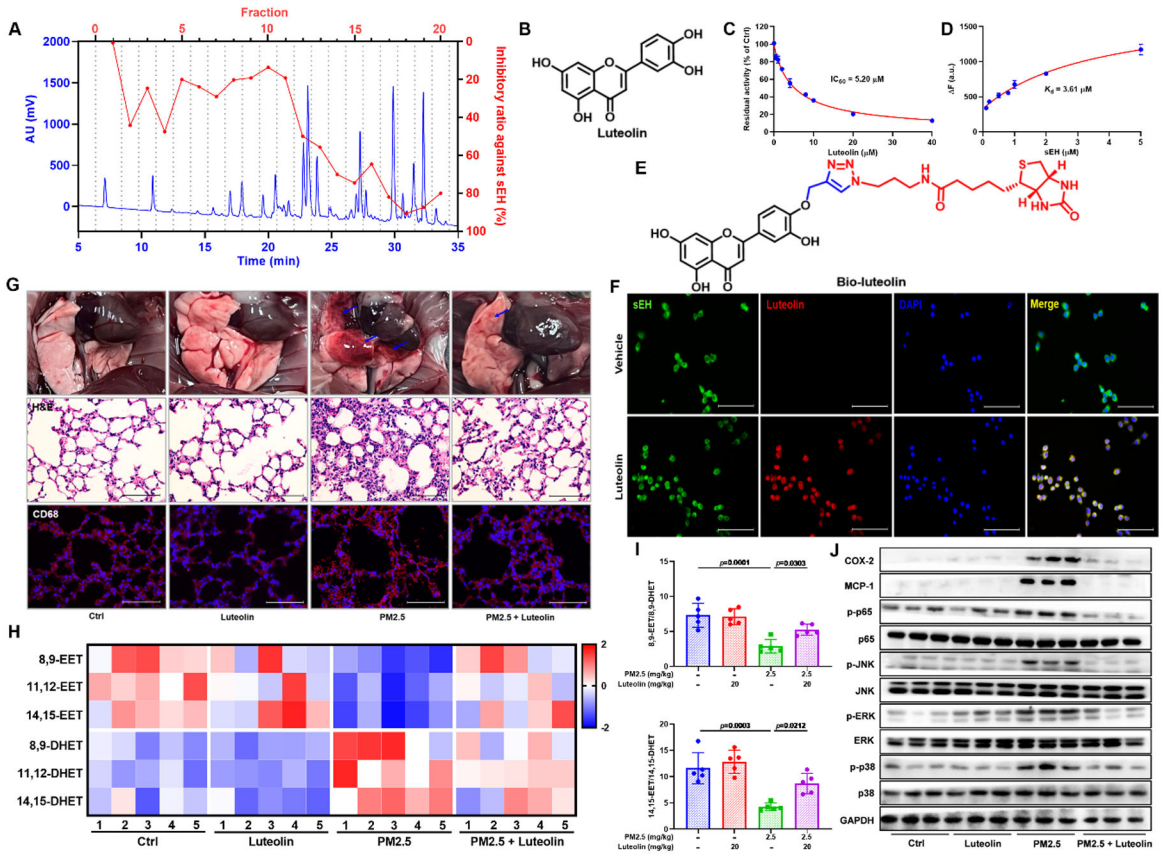

Figure 6. Luteolin from *I. japonica* ameliorated lung injury mediated by PM2.5.

(A) The pharmacodynamics plot of *I. japonica*. (B) The structure of luteolin. (C) Inhibitory effect of luteolin towards sEH (mean ± SEM, n = 3). (D) The binding capability of luteolin with sEH (mean ± SEM, n = 3). (E) The structure of luteolin couple with biotin (Bio-luteolin). (F) The co-location of luteolin with sEH. (G) Representative lung, H&E, and CD68 staining plots. (H) Heatmap plot. (I) The ratios of EETs and DHETs (mean ± SEM, n = 5, one-way ANOVA). (J) Effects of luteolin on proteins involved in the MAPK/NF-κB pathway.